X-RAY PHOTOEMISSION STUDY OF YTTRIUM CONTAINED IN RADIOTHERAPY SYSTEMS

V. Simon[*], D. Eniu[a], A. Takács[b], K. Magyari, M. Neumann[b], S. Simon

Babes-Bolyai University, Faculty of Physics, 400084 Cluj-Napoca,Romania
[a]University of Medicine and Pharmacy, Faculty of Pharmacy, 400010 Cluj-Napoca, Romania
[b]University of Osnabrück, Physics Department, 49069 Osnabrück, Germany

X-ray photoelectron spectroscopy was used to obtain information on yttrium local atomic arrangement and electronic structure in Y_2O_3-Al_2O_3-SiO_2 glass system doped up to 1 mol % with Fe_2O_3. Both Y 3p and Y 3d core level photoelectron peaks are influenced by iron addition to yttrium alumino-silicate host glass and evidence spin orbit splitting. The positions of the photoelectron peaks are shifted to some higher energies relative to pure yttrium. This is correlated with fact that the effective electronic charge density on the yttrium cations decreases as the number of oxygen anions increases. The decrease in effective electronic charge density around yttrium would be reflected in an increase in the binding energy of the remaining electrons.

1. Introduction

Yttrium aluminosilicate glasses have lead to a special family of glasses used in radiotherapy [1]. Among the oxide materials that are specially developed for medical use, glasses for radiotherapy and hyperthermia are also included. Glasses are used for internal radiotherapy of cancer as radioactive microspheres. The radioisotope Y-90 can be activated by neutron irradiation of the initial isotopic stable glasses. The advantage of using these radiation carriers in relation to the conventional external beam radiotherapy is that much larger doses of radiation can be safely delivered to the target site, eliminating exposure to other parts of the body.

The application of yttrium oxide aluminosilicate glasses in the cancer therapy could be extended from internal radiotherapy to hyperthermia therapy [2] by addition of iron oxide to yttrium aluminosilicate glass composition. The surface properties influence the biomaterials behaviour in the human body and depend on the local atomic arrangement. Spectroscopic techniques like X-ray photoelectron spectroscopy become an important tool in the study of the local structure of oxide glasses [3,4].

The present study is focussed on the investigation of electronic structure and implicitly local order changes around yttrium atoms in yttrium aluminosilicate glasses doped with iron.

2. Experimental

Glass samples belonging to $17Y_2O_3 \cdot 19Al_2O_3 \cdot (64-x)SiO_2 \cdot xFe_2O_3$ system ($0 \leq x \leq 1$ mol %) were obtained using oxides of reagent grade purity. Calculated amounts of the oxide powders were mixed and melted in sintercorundum crucibles at 1550 °C for 30 minutes. The samples were obtained by fast quenching of the melts cast and pressed between steel plates at room temperature.

---

[*] Corresponding author: viosimon@phys.ubbcluj.ro

XPS measurements were performed using a PHI 5600ci Multi Technique system with monochromatised Al K_{α} radiation from a 250 W X-ray source (hv = 1486,6 eV). During the measurements the pressure in the analysis chamber was in the 10^{-9} Torr range. Low energy electron beam was used to achieve charge neutrality at the sample surface. The absolute binding energies of Y 3d and Y 3p photoelectron peaks were determined by referencing to the C 1s transition at 284.6 eV that results most probably during the measurements from adsorbed species. The position and full width at half maximum of photoelectron peaks were estimated using spectra simulation based on summation of lorentzian and gaussian functions.

3. Results and discussion

The vitreous state of $17Y_2O_3 \cdot 19Al_2O_3 \cdot (64-x)SiO_2 \cdot xFe_2O_3$ samples was confirmed by X-ray powder diffraction analysis that did not evidence any crystalline phase. The diffraction patterns consist of a very large peak typical for glass systems.

Pure silica glass is a prototype of a network forming glass. Its very high melting temperature can be reduced by addition of modifier oxides. The modifier oxides cause the network to break. The mechanism of this incorporation mainly depends upon the valence state and the coordination of the glass former and modifier elements. In the pure silica glass there are many small rings that produce a complex and quite rigid three-dimensional network. Opening this network up and altering the ratio between the number of silicon and oxygen atoms produce changes in the local structure and implicitly in the melting temperature.

There are several criteria for predicting the role of the oxides in a glass by considering and comparing the characteristic parameters of the entering cations. In Table 1 are given ionic radius, coordination type, ionic field strength, single bond strength with oxygen and electronegativity of the cations from the investigated glasses [5,6,7]. The cationic field strength is expressed by the ration of the cation charge to the square of the ionic radius. The cations belonging to the conventional glass former oxides are characterised by high field strengths as compared to the cations entering as modifiers. In this approach, one remarks (Table 1) that in the investigated system Al_2O_3, Fe_2O_3 and particularly Y_2O_3 are expected to play the role of modifier oxides in the silicate glass network built up from tetrahedral $[SiO_4]$ structural units.

Table 1. Coordination number, field strength, Pauling electronegativity and single bond strength for the cations entering in $17Y_2O_3 \cdot 19Al_2O_3 \cdot (64-x)SiO_2 \cdot xFe_2O_3$ glasses.

Cation	Coordination number	Shannon ionic radius (Å)	Cation field strength ($Å^{-2}$)	Electro-negativity (Pauling units)	Single bond strength M-O (kJ·mol^{-1})
Si^{4+}	4	0.40	25	1.90	799.6 ±13.4
	6	0.54	13.72		
Al^{3+}	4	0.53	10.68	1.61	511 ±3
	6	0.675	6.58		
Y^{3+}	6	1.04	2.77	1.22	719.6 ±11.3
	8	1.159	2.23		
Fe^{3+}	4 tetrahedral	0.63	7.56	1.83	390.4 ±17.2
	6 octahedral	0.69	6.30		
	8	0.92	3.54		
Fe^{2+}	4 tetrahedral	0.77	3.37		
	4 square-planar	0.78	3.29		
	6 octahedral	0.75	3.56		
	6 octahedral, high spin	0.92	2.36		
	8	1.06	1.78		

Several techniques are employed in the attempt to identify the atomic environment of the different elements in glasses. X-ray photoelectron spectroscopy is used to obtain information from the photoelectron peaks corresponding to the component elements [8,9,10]. The binding energy is a measure of the extent to which electrons are localized on the atom or in the internuclear region and hence of the constraints on the network, as reflected by the physical properties. The terms network former, intermediate, and modifier, are therefore simply a reflection of this electron localization. A modifier cation has low electronegativity and forms ionic bonds and there is a transfer of electronic charge to the neighbouring oxygen.

In Fig. 1 are shown the high resolution Y 3d spectra. One can observe the iron doping influence on yttrium neighbourhood in the investigated samples. By inspecting the Y 3d photopeaks one remarks that they are not symmetric and for x = 0.2 and 0.5 is immediately observed the spin orbit splitting. On deconvolution they have been found to consists of two peaks each. The positions of the photoelectron peaks are shifted to some higher energies relative to pure Y $3 d_{5/2}$ (155.8 eV) and Y $3 d_{3/2}$ (157.7 eV). The spin orbit splitting appreciated for x = 0 and 1 from the deconvoluted spectra are little different from the well evidenced spin orbit splitting for the samples with x = 0.2 and 0.5 (Table 4). One considers that the areas under the lines corresponding to deconvoluted spectra could also reflect the differentiated influence of iron doping on the local order in their atomic environment containing yttrium.
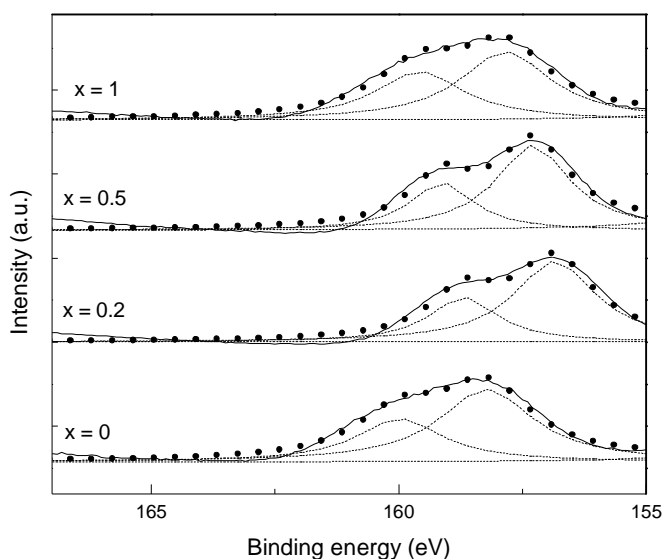

Fig. 1. Experimental and simulated Y 3d and Si 2s core level photoelectron spectra of $17Y_2O_3 \cdot 19Al_2O_3 \cdot (64-x)SiO_2 \cdot xFe_2O_3$ samples.

Table 4. Core level electron binding energies (BE), full-width at half-maximum (FWHM), spin orbit splitting and areas (A) under simulation lines for Y $3 d_{5/2}$, Y $3 d_{3/2}$ and Si 2s photoelectron peaks from $17Y_2O_3 \cdot 19Al_2O_3 \cdot (64-x)SiO_2 \cdot xFe_2O_3$ samples.

x (mol %)	BE (eV)		Spin orbit splitting (eV)	$A_{(Y3d)}$ (a.u.)
	Y $3 d_{5/2}$	Y $3 d_{3/2}$		
0	158.18	159.91	1.73	238.09
0.2	156.86	158.71	1.85	219.68
0.5	157.28	159.11	1.83	211.54
1	157.84	159.57	1.73	239.35

The Y 3p high resolution spectra (Fig. 2) present a spin orbit splitting close to 11.7 eV. The positions of the photoelectron peaks (Table 5) are shifted to some higher energies relative to pure Y $3 p_{3/2}$ (298.8 eV) and Y $3 p_{1/2}$ (310.6 eV).
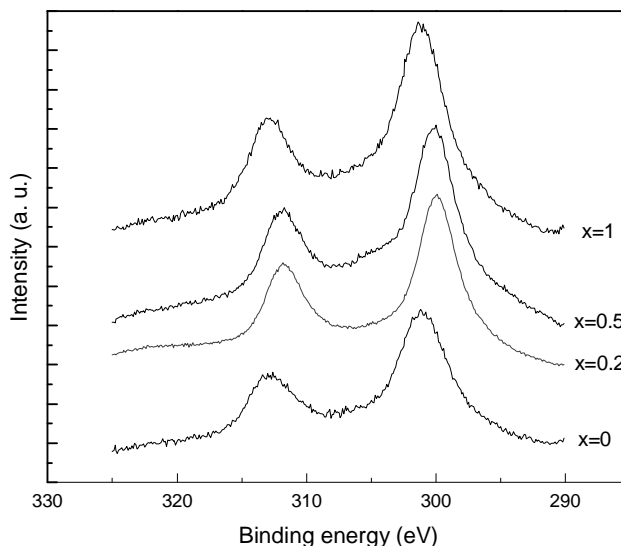

Fig. 2. Y 3p core level photoelectron spectra of $17Y_2O_3 \cdot 19Al_2O_3 \cdot (64-x)SiO_2 \cdot xFe_2O_3$ samples.

Relative to the host glass sample (x = 0) the binding energy of Y 3p photopeaks are slightly lower in the sample with x = 0.2 mol % Fe_2O_3, but the binding energy shift sensibly increases with the doping level.

Table 5 Core level electron binding energies (BE), full-width at half-maximum (FWHM), spin orbit splitting and areas under simulation lines for Y $3 p_{3/2}$ and Y $3 p_{1/2}$ photoelectron peaks from $17Y_2O_3 \cdot 19Al_2O_3 \cdot (64-x)SiO_2 \cdot xFe_2O_3$ samples.

x (mol%)	BE (eV)		FWHM (eV)		Spin orbit splitting (eV)	A (a.u.)	A (a.u.)	$A_{3/2}$ /$A_{1/2}$
	Y $3 p_{3/2}$	Y $3 p_{1/2}$	Y $3 p_{3/2}$	Y $3 p_{1/2}$		Y $3 p_{3/2}$	Y $3 p_{1/2}$	
0	301.17	312.95	5.29	5.27	11.68	285.17	146.19	1.95
0.2	300.03	311.80	3.51	4.56	11.77	239.46	158.29	1.51
0.5	300.13	311.80	4.90	6.21	11.67	360.78	238.76	1.51
1	301.18	312.86	5.13	5.85	11.68	416.95	241.66	1.73

The binding energies of Y 3p and Y 3d core level electrons after an initial decrease gradually change to higher values as the x value increases, since there is a deficiency in electron density around the Y atom, causing increase in binding energy of core level electrons. The partial transfer of electrons from Fe^{3+} to O^{2-} ions causes this chemical shift. This is correlated with fact that the effective electronic charge density on the yttrium cations decreases as the number of oxygen anions increases. The decrease in effective electronic charge density around the cations would be reflected in an increase in the binding energy of the remaining electrons.

According to the classical model of silicate glasses, the influence of the network modifier cations on the local structure consists in the compensation of the negative charges and is responsible for the disruption of the oxygen bridges in the silica network [11]. A network former has relatively high electronegativity, the bond to oxygen is more covalent, constraining the electron density to the region between the atoms and reducing the electron density on the oxygen atom. This results in an increased electron binding energy, which yields a bridging oxygen peak in the XPS spectrum. The

binding energy dependence on Fe_2O_3 content is similar with the evolution determined by addition of Pr_2O_3 to zinc borate glasses [12]. The iron doping effect is observed without doubt already for $x = 0.2$. Both binding energy and line width are modified: the binding energy is diminished and the line width is narrowed. By increasing the Fe_2O_3 doping content to 0.5 and 1 mol % binding energy and line width show an apparently linear increase.

4. Conclusions

The next nearest neighbours of the yttrium atoms are affected by iron doping of yttrium aluminosilicate glass host as evidenced by composition dependence of binding energies of yttrium core level electrons. The full width at half maximum indicates an ordering tendency in the local structure by iron addition to the host yttrium aluminosilicate glass. Progressive iron doping causes the decrease of the effective electronic charge density on yttrium cations.

References

[1] G. J. Ehrhardt, D. E. Day, Nucl. Med. Biol. **14**, 233 (1987).
[2] S. Atalay, H. I. Adiguzel, F. Atalay, Mater. Sci. Eng. A **304**, 796 (2001).
[3] I. A. Gee, D. Holland, C. F. McCoville, Phys. Chem. Glasses **42**(6), 339 (2001).
[4] V. Simon, H. Bako-Szilagyi, M. Neumann, S. G. Chizbaian, S. Simon, Mod. Phys. Lett. B, **17** (7), 291 (2003).
[5] R. D. Shannon, Acta Cryst. **A32**, 751 (1976).
[6] J. E. Huheey, E. A. Keiter, R. L. Keiter in Inorganic Chemistry: Principles of Structure and Reactivity, 4th edition, Harper Collins, New York, USA, 1993.
[7] J. A. Kerr in CRC Handbook of Chemistry and Physics, D.R. Lide, (ed.) CRC Press, Boca Raton, Florida, USA, 81-st ed., 2000.
[8] S. Matsumoto, T. Nanba, Y. Miura, J. Ceram. Soc. Japan **106**, 415 (1998).
[9] R. K. Brow, R. J. Kirkpatrick, G. Turner, J. Am. Cer. Soc. **73**, 2293 (1990).
[10] T. Honma, R. Sato, Y. Benino, T. Komatsu, V. Dimitrov. J. Non-Cryst. Solids **272**, 1 (2000).
[11] E. Muller, K. Heide, E. D. Zanutto, Zeitschrift für Kristallographie **200**, 287 (1992).
[12] S. K. Lee, J. F. Stebbins, American Mineralogist **84**, 937 (1999).